











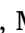





Shaping gas exchange under drought: Seasonal and interspecific variation in photosynthetic traits of *Pinus halepensis* and *Pinus brutia* in Mediterranean forests

Natasa Kiorapostolou^{a,*,1} , Nikoleta Eleftheriadou^{b,1} , Christodoulos Sazeides^c , Nikos Markos^a , Alexandros Gouvas^b , Evdoxia Bintsi-Frantzi^c , Efstathia D. Mantzari^c , Georgios Xanthopoulos^a , Panayiotis G. Dimitrakopoulos^c , Nikolaos M. Fyllas^d , Gavriil Spyroglou^a , Kalliopi Radoglou^b , Rossella Guerrieri^e , Mariangela N. Fotelli^a 

^a Forest Research Institute, Hellenic Agricultural Organization Dimira, Thessaloniki 57006, Greece

^b Department of Forestry and Management of Environment and Natural Resources, Democritus University of Thrace, Orestiada 68200, Greece

^c Biodiversity Conservation Laboratory, Department of Environment, University of the Aegean, Mytilene 81132, Greece

^d Department of Biology, National and Kapodistrian University of Athens, Athens 15701, Greece

^e Department of Agricultural and Food Sciences, University of Bologna, Bologna 40127, Italy

ARTICLE INFO

Keywords:

Aleppo pine
Calabrian pine
Photosynthesis
Stomatal regulation
Seasonality
VPD
LSWI

ABSTRACT

As Mediterranean pine forests are increasingly exposed to intense drought events that may threaten their survival, it is important to improve our understanding of their ecophysiological responses to climatic drivers under different temporal and spatial scales. We studied key photosynthetic traits in different ecosystems of *Pinus halepensis* and the less studied *Pinus brutia* by applying an integrated, multi-site and multi-season comparative approach. For this purpose, we performed seasonal gas exchange measurements across three sites (Lesvos, Sani, and Xanthi) and ten plots in Greece to assess how species-specific stomatal strategies, microclimatic drivers, and stand structure shape carbon assimilation. We assessed CO₂- and light-saturated photosynthetic capacity (A_{max}), stomatal conductance (g_s), and intrinsic water use efficiency (iWUE), and their responses to vapor pressure deficit (VPD) and the land surface water index (LSWI). No effect of stand structure, but significant variation among sites and seasons in A_{max} , g_s , and iWUE was detected. *P. halepensis* in Sani and *P. brutia* in Xanthi exhibited a bimodal photosynthetic activity, showing the highest A_{max} in spring and its recovery in autumn or winter under favorable microclimate, reflecting an adaptive strategy to exploit favorable microclimatic windows. *P. brutia* in Lesvos, characterized by the highest VPD, exhibited a more conservative seasonal pattern with a peak of A_{max} only in spring, reflecting prolonged atmospheric constraints on stomatal opening. Overall, atmospheric drought vs. land surface water availability had a stronger control on the A_{max} of both species, reflecting a prioritization of hydraulic safety, in which both species employ isohydric stomatal regulation to increase their intrinsic water use efficiency at the cost of carbon uptake. However, *P. brutia* showed a less steep decline in A_{max} under high atmospheric water demand, indicating a less isohydric response than *P. halepensis* that allows the maintenance of photosynthetic activity over a wider range of VPD and offers an advantage under increasingly intensified drought regimes.

1. Introduction

Photosynthesis is a fundamental physiological process through which plants assimilate atmospheric carbon dioxide (CO₂) using the

energy from sunlight to synthesize carbohydrates that are used to support growth, reproduction, and maintenance. Photosynthetic capacity, typically captured by light-saturated assimilation rates, and stomatal conductance are sensitive to both short-term environmental fluctuations

* Corresponding author.

E-mail address: nkiorapostolou@elgo.gr (N. Kiorapostolou).

¹ Equal Author contribution

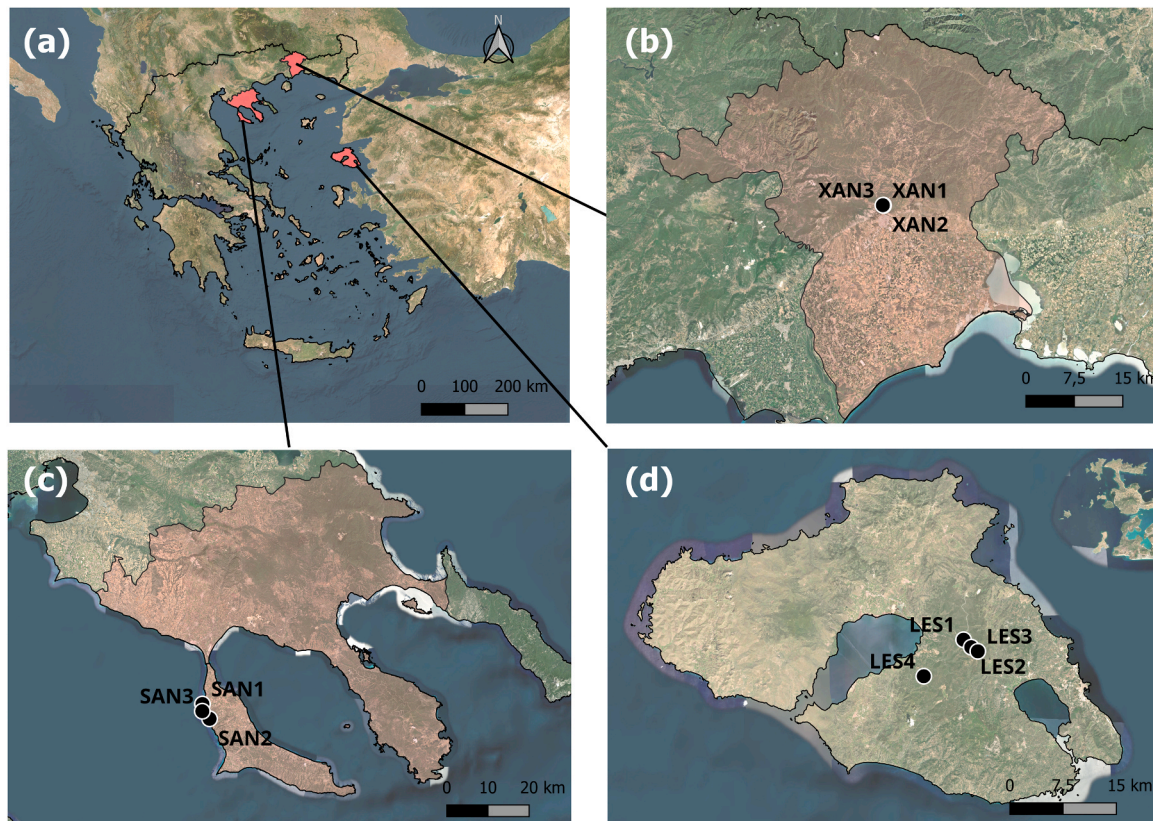


Fig. 1. Study sites' location in northern Greece (a) and the monitoring plots at each site, in Xanthi (b), Sani (c), and Lesvos (d).

and long-term acclimation processes (Flexas et al., 2013; Lawson and Blatt, 2014; Miner et al., 2017; Niinemets, 2010). These parameters may be further shaped by needle age, sunlight status, and microclimate, making them integrative indicators of the trees' physiological status (Warren, 2008). Natural terrestrial ecosystems, such as mature forests, are considered important carbon sinks, but their efficiency in terms of carbon sequestration is greatly controlled by their adaptation to a changing climate. At the plant level, carbon assimilation is shaped by stomatal regulation and the interplay between water and carbon balance. Trees regulate gas exchange and water loss via stomatal control to maintain hydraulic functionality, while also supporting growth and metabolic demand (Martínez-Vilalta and García-Forner, 2017). Strategies in stomatal regulation along the isohydric-anisohydric continuum play a key role in this balance, with isohydric species prioritizing hydraulic safety, closing stomata earlier, and anisohydric species maintaining stomatal opening, favoring carbon gain even under warmer and drier conditions (Martínez-Vilalta et al., 2014; Kiorapostolou et al., 2018).

Pinus halepensis Mill. and *Pinus brutia* Ten. cover the western and eastern parts of the Mediterranean basin, respectively, while their transition zone is found in Greece, where both species coexist (Chambel et al., 2013). The forest ecosystems formed by these two pine species are extensively distributed, covering approximately 7 million ha (Chambel et al., 2013), from the sea level up to 600 m in elevation. Management of Mediterranean low-elevation pines varies from none to mild overstory thinning and partial understory removal, based on regional priorities. These forests contribute substantially to climate change mitigation (del Río et al., 2017), but their efficiency in carbon storage may vary with age and forest management (Moreno-Fernandez et al., 2015; Navarro-Cerrillo et al., 2022). Moreover, with ongoing climate change, the carbon sink capacity of these ecosystems may be at risk (Peñuelas et al., 2017; Sarris et al., 2007), underlining the importance of understanding how shifting climate conditions could impact their carbon

dynamics.

Climate models predict that periods of drought and increased temperatures will be prolonged and intense in the near future (IPCC, 2023), and this is particularly true for the eastern Mediterranean basin (Lazoglou et al., 2024). Increasing temperature and VPD affect leaf gas exchange through reduction of stomatal conductance and metabolic limitation of photosynthesis (Farquhar and Sharkey, 1982; Zhou et al., 2013). Under increased atmospheric drought (high VPD), pine trees close their stomata to limit water loss, which drastically reduces photosynthetic CO₂ uptake (Birami et al., 2018; Tatarinov et al., 2016; Warren et al., 2004). Both *P. halepensis* and *P. brutia* follow an isohydric strategy, closing stomata early during summer droughts to conserve water and avoid hydraulic failure, leading to low carbon uptake during the driest periods (Cherif et al., 2019; Fotelli et al., 2019, 2020; Houminer et al., 2022; Klein et al., 2011; Markos et al., 2024). Under prolonged drought, this water-saving mechanism may lead to reduced growth and, finally, mortality. Growth decline and increasing mortality rates have been reported for both *P. halepensis* and *P. brutia* after consecutive dry years (Alsanousi et al., 2025; Christopoulou et al., 2022;). In addition, model simulations predict a sharp decline in net ecosystem productivity of *P. brutia* forests under future climate scenarios, compared to the present climatic conditions (Sazeides and Fyllas, 2025).

Despite these similarities of *P. halepensis* and *P. brutia* in terms of their responses to drought, assessing if the two species differ in their degree of isohydric regulation is important for effectively predicting their future behavior under the changing climate. However, such comparative physiological studies are scarce. In a recent study, *P. halepensis* has been shown to exhibit a more pronounced and rapid reduction in stomatal conductance and transpiration under drought, compared to *P. brutia* (Houminer et al., 2022), indicating a stricter expression of isohydric behavior. Furthermore, we need to advance our understanding of how the photosynthetic traits of the two pine species,

Table 1
 Characteristics of the permanent monitoring plots at the three study sites (Lesvos, Sani, Xanthi). Soil texture abbreviations: CL: Clay, SCL: Sandy Clay Loam, S: Sandy, C: Clay, SL: Silt Loam, LS: Loamy sand.

Species	Site	Plot	Longitude	Latitude	LAI *	Basal area (m ² /ha)	Age	Tree DBH (cm)	Tree height (m)	Soil texture	Soil pH	Origin	Management
<i>P. brutia</i>	Lesvos	LES1	26.36179	39.17160	1.06	9.69 ± 3.86	20	7.36 ± 3.99	3.34 ± 1.15	CL	6.7	Natural post-fire regeneration	None
		LES2	26.29545	39.12662	1.66	22.2 ± 5.48	46	8.90 ± 5.93	4.68 ± 2.69	SCL	6.6		
		LES3	26.38450	39.15641	2.13	31.8 ± 9.09	78	28.99 ± 7.02	11.31 ± 2.04	SCL	6.6		
<i>P. halepensis</i>	Sani	LES4	26.37402	39.16189	2.5	31.2 ± 8.54	97	38.6 ± 13.85	16.22 ± 4.50	SIL	7.1	Natural forest	None (low density)
		SAN1	23.31355	40.1085	2.14 (1.88)	23.5 ± 15.7	85	40.5 ± 15.66	14.96 ± 4.77	S	7.6		Understory removal
		SAN2	23.33419	40.07637	2.29	27.4 ± 7.58	64	28.2 ± 7.58	15.66 ± 4.45	C	7.2		None (high density)
<i>P. brutia</i>	Xanthi	SAN3	23.31331	40.09282	3.06 (4.76)	25.3 ± 7.10	72	26.5 ± 7.03	15.15 ± 1.94	SCL	7.1	Planted forest	None
		XAN1	24.88772	41.15615	1.29	49.3 ± 16.2	72	35.8 ± 8.23	20.35 ± 2.85	SL	6.1		Moderate thinning
		XAN2	24.88650	41.15597	1.38	43.3 ± 12.5	72	30.19 ± 5.42	16.76 ± 2.84	LS	6.2		Intensive thinning
		XAN3	24.88765	41.15548	0.73	36.3 ± 11.2	72	22.7 ± 6.14	17.76 ± 3.89	SL	5.6		

(*) in plots SAN1 and SAN3 the LAI of the understory shrub vegetation is given in parentheses.

particularly the less studied *P. brutia*, change under different stand structures and across spatial and temporal scales in relation to both atmospheric water demand and soil and vegetation water content, in order to effectively plan their climate-smart management.

In this research, we measured photosynthesis and stomatal conductance of *P. halepensis* and *P. brutia* in three distinct Mediterranean sites in Greece during an entire year. We aimed at assessing the variation in photosynthetic capacity across stands of different structure, sites, seasons, and species, and at understanding the role of atmospheric and soil drought (as imprinted in VPD and LSWI, respectively) in controlling the coupling between needle carbon and water balance in these typical semi-arid pine ecosystems. We hypothesized that gas exchange traits would exhibit a bimodal seasonal pattern with photosynthetic recovery driven by favorable microclimatic windows. We also expected similar drivers for photosynthetic capacity and intrinsic water use efficiency between *P. halepensis* and *P. brutia*, but we focused on identifying differences in the isohydric response of the two species.

2. Materials and methods

2.1. Study sites and monitoring plots

We focused on three study sites representing typical low-elevation Mediterranean pine forests in Greece, i.e., Lesvos and Xanthi dominated by *P. brutia* and Sani dominated by *P. halepensis* (Fig. 1). At Lesvos, no understory vegetation is present, at Sani there is an understory shrub layer (0.5–2.0 m height) consisting mainly of *Pistacia lentiscus*, *Phillyrea latifolia*, and *Quercus coccifera*, and in Xanthi, there is an at least 5 m-high layer below the pines, consisting of deciduous broadleaf trees (mainly *Carpinus orientalis*, *Fraxinus ornus*, *Quercus coccifera*, *Quercus frainetto*). Varying forest management practices, stand age and microclimate have shaped pine stands of different structures. To account for this variability, we selected 3–4 representative plots at each site (in total 10 monitoring plots) and their soil, tree, and stand characteristics were systematically measured (Table 1). Basal Area and Leaf Area Index (LAI) reflect the between-plot differences in stand structure. A fully harmonized monitoring protocol was implemented across the 10 plots, as described in Eleftheriadou et al. (2026).

LAI was determined with a ceptometer (Accupar LP-80; Decagon Devices Inc, WA, USA), by systematically measuring photosynthetic active radiation (PAR) at 36 points above the forest floor (1.3 m) and comparing each PAR with that measured outside of the canopy under full light conditions. All LAI measurements were made around solar noon, and the leaf distribution parameter was set to X = 1.

In addition, the microclimatic conditions of the plots were continuously recorded and are shown in Fig. 2. In each plot, an air temperature and relative humidity sensor (MX2031A, Hobo, Onset, USA) was installed at c. 2 m height, at the forest understory, and a soil moisture and temperature sensor (MX230x, Hobo, Onset, USA) was placed at 5 cm depth. Mean daily values were estimated from 30-min interval records. However, because soil moisture measured at 5 cm depth only reflects the superficial soil water, we additionally used the Land Surface Water Index (LSWI) as a representative indicator of overall ecosystem water status in Mediterranean pine ecosystems (Markos et al., 2024). The index was estimated for the corresponding period of measurement for each plot separately, using Sentinel 2 msi L2A products. Data was extracted through the Copernicus EO Browser (<https://browser.dataspace.copernicus.eu>), as mean values of the polygons that covered the area of each plot. LSWI values were estimated for clear days (cloud cover=0), while raw images were checked again for potential algorithm failures.

2.2. Tree selection and performance of needle gas exchange measurements

Four (4) healthy, dominant, and non-neighboring pine trees were selected and marked in each plot. In Sani, two of the initially selected

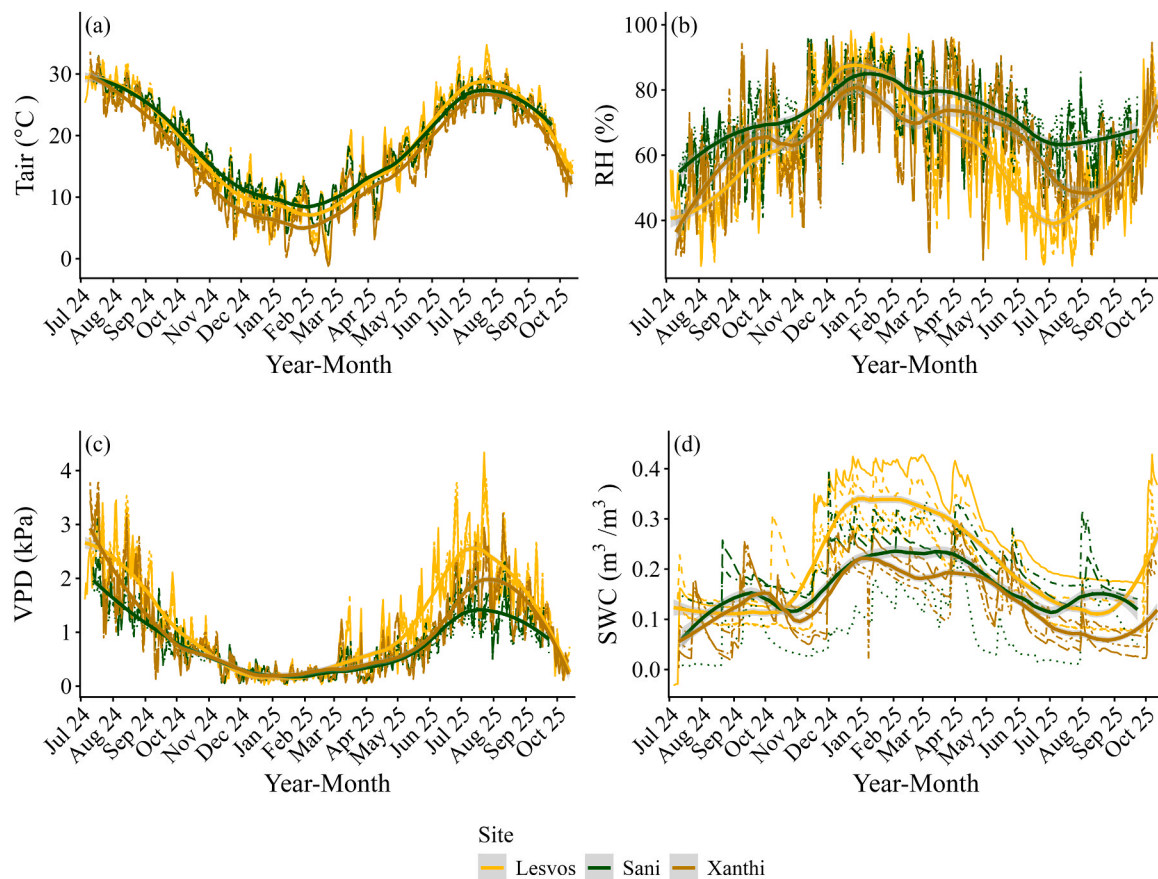


Fig. 2. Climatic variables in Lesvos, Sani, and Xanthi across the seasons during the study period. Tair (a), RH (b), VPD (c), and SWC (d) stand for air temperature, air relative humidity, vapor pressure deficit, and soil water content, respectively. Solid lines represent the mean seasonal variation per study site and dashed lines show the variation of each monitoring plot.

trees in plot SAN3 were replaced with trees of similar age and DBH in April 2025, due to observed infestation. On each tree, gas exchange measurements were conducted once per season, starting from summer 2024 and ending in summer 2025, using portable gas exchange systems (for Xanthi: CIRAS-3; PP Systems, Amesbury, MA, USA, and for Sani and Lesvos, Li6400XT and Li6400, respectively; Licor, Nebraska, USA). To ensure consistency in gas exchange measurements between the CIRAS and Licor devices, we used identical settings and performed response curves of net photosynthetic rate (A_{net} , $\mu\text{mol m}^{-2} \text{s}^{-1}$) to photosynthetically active radiation (PAR), which showed no differences (Figure S1).

Considering the local climatic conditions, measurements were performed during non-windy or rainy days, within the same 4-week time window at all sites, and the same 1-week window at all plots per site. Two branches were sampled per tree: a fully sunlit one, from the upper canopy of the tree, and a shaded one from the lower canopy to account for the variability in light conditions within the canopy. Based on the methodology applied by Fyllas et al. (2017), (2020) and Fotelli et al. (2020), branches were collected using a telescopic pruner of 6 or 20 m, depending on tree height. Immediately after cutting, branches were placed in a bucket of water and recut underwater to prevent xylem embolism. Current-year needles or, when not fully developed, needles from the previous year were selected for measurement. Three pairs of healthy needles were carefully placed in the chamber without overlapping. When the chamber area was not fully covered by needles, the part of the needles enclosed within the chamber was marked, its area was measured using the image analysis software ImageJ (Schneider et al., 2012), and photosynthesis values were corrected accordingly.

In each plot, we performed eight (8) photosynthesis light response

curves (two per selected tree), starting early in the morning, at around 8:00 a.m., and ending at least two hours before sunset. Average curves per plot are depicted in Figure S2. A random rotation between trees was applied during each season to exclude daytime effects on gas exchange. During each curve, the chamber air flow rate was set to $500 \mu\text{mol air s}^{-1}$, and the reference CO_2 concentration was maintained at 420 ppm. The block temperature of the chamber was set equal to the ambient temperature. Relative humidity (RH) inside the chamber was either matched to ambient conditions when RH was 40–60 % or set to 70 % of the external relative humidity when ambient RH was higher during humid days. Initial needles' acclimation was conducted at PAR equal to $1000 \mu\text{mol m}^{-2} \text{s}^{-1}$ for shaded needles and $1600 \mu\text{mol m}^{-2} \text{s}^{-1}$ for the sunlit ones. Equilibrium was considered achieved when stomatal conductance exceeded $0.02 \text{ mol m}^{-2} \text{s}^{-1}$ and stabilized, or when transpiration rates exceeded $0.11 \text{ mmol m}^{-2} \text{s}^{-1}$ for shaded needles and $0.12 \text{ mmol m}^{-2} \text{s}^{-1}$ for sunlit needles. Light response curves were performed by sequentially adjusting PAR to the following values: 2000, 1800, 1600, 1400, 1200, 1000, 800, 600, 400, 200, 100, 80, 60, 40, 20, and $0 \mu\text{mol m}^{-2} \text{s}^{-1}$. For each PAR level, after allowing the needles to reach equilibrium, three recordings of A_{net} were made. All settings and calibration protocols followed standard manufacturer guidelines and were consistent across sampling sites and dates.

The CO_2 and light-saturated photosynthetic capacity (A_{max}) was calculated with the modified non-rectangular hyperbola equation as described by Markos and Kyparissis (2011), which takes into account the initial quantum yield, the curvature of the response, and the light-saturated asymptote of net photosynthesis. This formulation was selected because it yields physiologically realistic A_{max} estimates, particularly in cases where light-response curves do not exhibit a clear

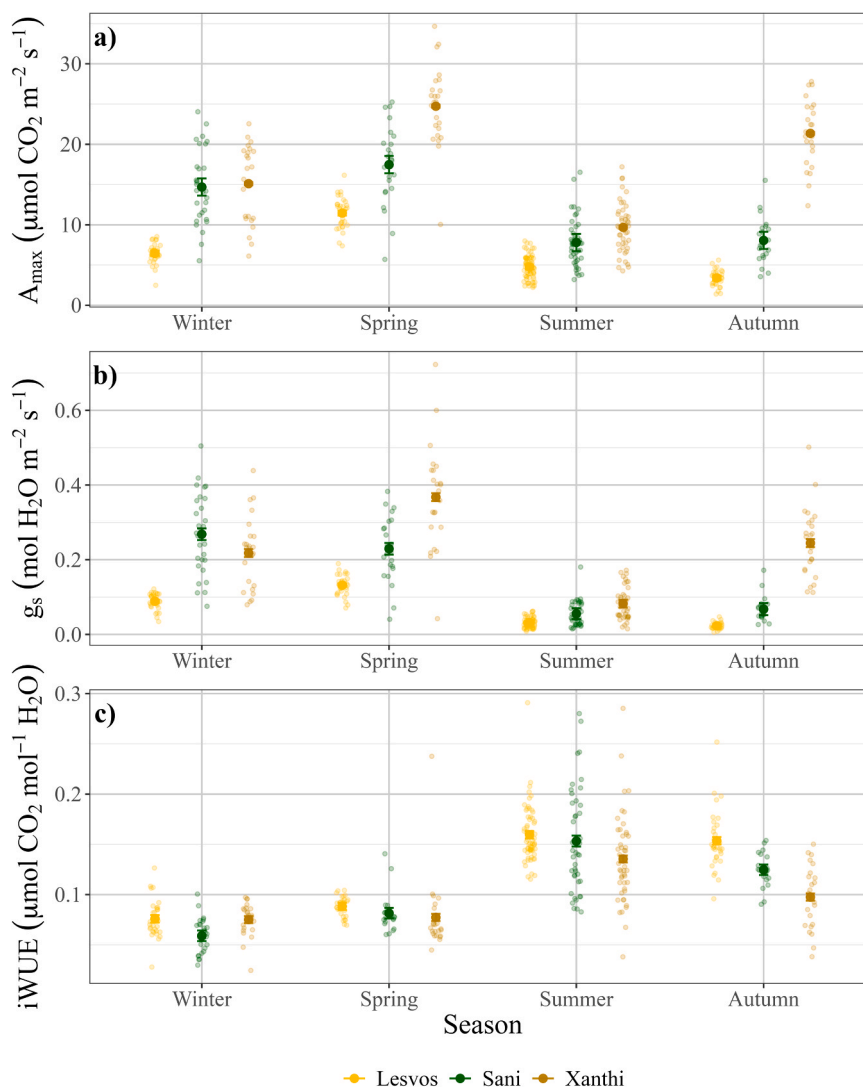


Fig. 3. Seasonal variation in photosynthetic capacity (A_{max} ; a), stomatal conductance (g_s ; b), intrinsic water use efficiency ($iWUE$; c) averaged over the three study sites. Background dots represent the raw data; foreground dots are the mixed model fitted mean \pm Standard Deviation.

light-saturation point. Although this model does not explicitly capture light suppression under very high irradiance, in comparison to alternative models that better capture such processes (e.g., Jin et al., 2024), such conditions were not observed in our measurements. In contrast, incomplete light saturation was frequently observed, making the MNRH model appropriate for our study. While A_{max} represents the potential photosynthetic capacity under saturating light and CO_2 , repeated measurements based on our protocol were used to capture A_{max} variability across seasons and sites, in accordance with previous studies (Fotelli et al., 2020; Sazeides et al., 2021). A_{max} showed no significant difference between sunlit and shaded needles (Figure S3) and, thus, the mean tree A_{max} was built as an average of both needles' categories. In addition, stomatal conductance (g_s) and leaf-to-air VPD (VPD) were calculated from the light response curves of both sunlit and shaded needles for $PAR > 1500 \text{ mol m}^{-2} \text{ s}^{-1}$. Intrinsic Water Use Efficiency ($iWUE$) was calculated as the ratio of A_{max} to g_s .

2.3. Midday needle water potential (Ψ_{midday})

Measurements of midday needle water potential were performed once, in late summer 2025, and before the first autumn rain event, to capture the minimum Ψ_{midday} values after the prolonged summer drought period. Assessments were performed on needles collected from

branches selected for the photosynthesis measurements using a pressure chamber (Model 1000, PMS, Instrument Company, Albany, OR, USA). Measurements were taken at midday (between 12:00 and 15:00), and after covering the needles with aluminum foil and placing them inside a polybag to avoid desiccation.

2.4. Statistical analysis

To account for the nested experimental design, we ran separate Linear Mixed Effect Models for A_{max} , g_s , and $iWUE$ as response variables. Initially, several stand and leaf-level parameters were included as covariates (Leaf Area Index; LAI, Basal Area; BA, soil Nitrogen concentration; N, soil Phosphorus concentration; P). An elimination procedure was followed, where non-significant terms were stepwisely removed until the final models were reached. Model performance was evaluated using marginal and conditional R^2 values, and considering the value of the model's Akaike Information Criterion (AIC). Fixed effects of the final models included site, season, VPD, and LSWI. To investigate site-specific and species-specific sensitivities, interaction terms were included. All statistical analyses were performed using R version 4.4.1 (R Core Team, 2024), using the packages "lme4" (Bates et al., 2015) and "lmerTest" (Kuznetsova, Brockhoff and Christensen, 2017).

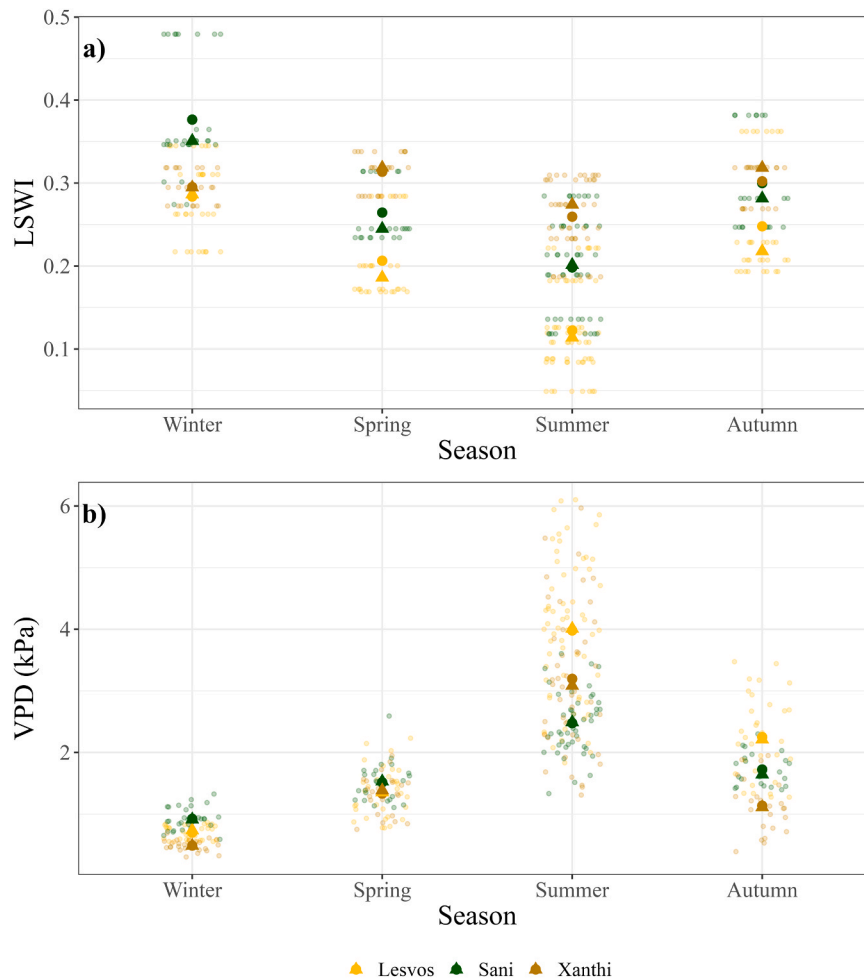


Fig. 4. Seasonal variation in Land Surface Water Index (LSWI; a) and Vapor Pressure Deficit (VPD; b) averaged over the three study sites. Dots represent the raw data; filled points represent the mean, and filled triangles represent the median values.

3. Results

3.1. Spatial and temporal differences in gas exchange, microclimate and Ψ_{midday}

No significant differences were detected in gas exchange parameters between the plots at any study site (Tables 2, 3, S2), indicating the lack of stand structure effects on needle gas exchange. On the contrary, strong seasonal control on all traits was observed (Fig. 3). A_{max} and g_s showed the same significant seasonal variation (Fig. 3a,b), with the highest A_{max} and g_s values observed in spring. However, *P. halepensis* in Sani and *P. brutia* in Xanthi demonstrated a bimodal pattern, by presenting also high A_{max} and g_s in winter and in autumn, respectively (Fig. 3a,b). Such a response was not observed with *P. brutia* in Lesvos, where A_{max} and g_s were significantly lower in all other seasons, compared to spring (Fig. 3a,b). Spatial differences were observed among sites, with Lesvos consistently exhibiting the lowest A_{max} and g_s while Xanthi showed the highest values, particularly in spring and autumn (Fig. 3a,b). Mixed-effect model analysis confirmed that these differences were strongly season-dependent, as indicated by significant site \times season interactions (Tables S1, S2).

iWUE and VPD exhibited the same seasonal fluctuation (Figs. 3c, 4b), with iWUE being highest in autumn and summer, and substantially lower during winter and spring. Mixed-effect models confirmed significant seasonal increases in iWUE during summer and autumn (Table 3). In addition, iWUE and VPD were higher in Lesvos, compared to Sani and Xanthi (Figs. 3c, 4b). LSWI was higher in winter and autumn, followed

by spring, and summer, which showed the lowest values. In addition, the lowest values were observed in summer in Lesvos (Fig. 4a).

Ψ_{midday} varied across sites with the most negative values observed in *P. brutia* in Lesvos (-3.69 ± 0.26 MPa) and Xanthi (-2.88 ± 0.22 MPa), compared to *P. halepensis* in Sani (-2.81 ± 0.14 MPa).

3.2. Drivers of A_{max} and iWUE

The final model for A_{max} (Marginal $R^2 = 0.793$) revealed significant main effects of VPD ($p = 0.005$), LSWI ($p = 0.026$), Site, and Season (Fig. 5a,b; Table 2). A significant interaction was found between VPD and site for Sani ($p = 0.002$). *P. halepensis* at Sani showed a much steeper slope in the relationship of A_{max} vs. VPD (slope = -3.59) compared to *P. brutia* at Lesvos (slope = -0.95) and Xanthi (slope = -0.84). In contrast, g_s did not exhibit significant main effects in relation to either VPD or LSWI and was, therefore, not retained in the final models.

As regards iWUE, the selected model indicated a significant overall increase with VPD ($p = 0.002$) (Fig. 6a,b; Table 3). However, the interaction between VPD and site for Sani was not significant ($p = 0.136$), suggesting that the response of iWUE to atmospheric drought was relatively stable at this site. In contrast, *P. brutia* at Xanthi showed a significantly different and more pronounced increase in iWUE with VPD ($p = 0.003$).

4. Discussion

P. halepensis and *P. brutia* are dominating low-elevation

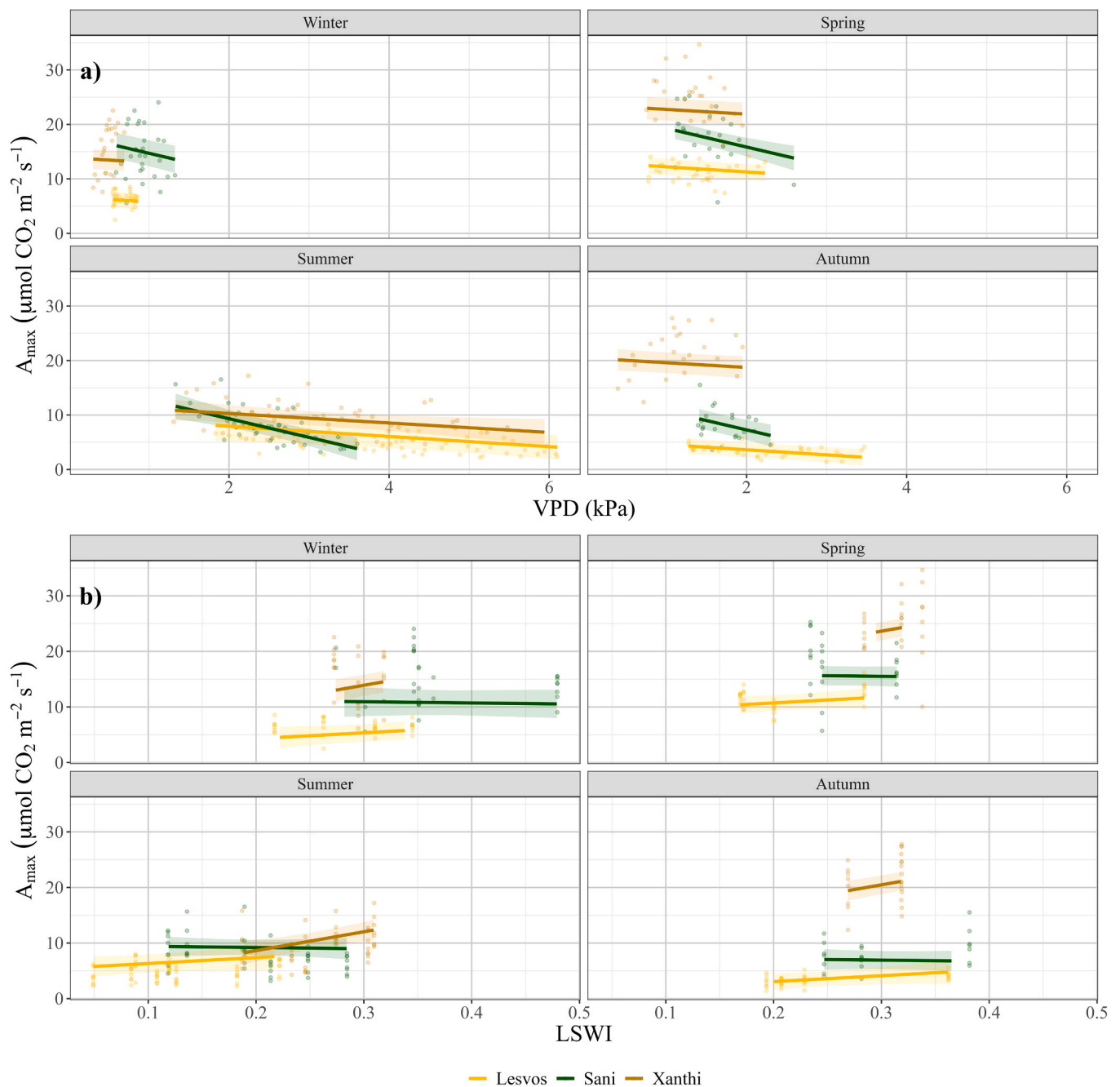


Fig. 5. Relationship between photosynthetic capacity (A_{max}) and VPD (a) and A_{max} and LSWI (b). Background dots represent the raw data; lines are from the fixed-effect model output and 95 % Confidence Interval ribbons.

Mediterranean pine ecosystems, providing multiple ecosystem services, such as climate regulation. These ecosystems are considered adapted to the semi-arid conditions of the eastern Mediterranean basin, but an in-depth understanding of their ecophysiological responses under the already exacerbating heat and drought periods is crucial in the light of global change. While more information is available about the photosynthetic patterns of *P. halepensis*, quite less is known about *P. brutia*. By measuring interannual gas exchange traits in *P. halepensis* and *P. brutia*, we aimed at exploring seasonal and spatial patterns and understanding gas exchange responses of these Mediterranean pines to xerothermic conditions across a gradient of three study sites in Greece, i.e., Lesvos, Sani, and Xanthi, characterized by different climatic conditions. In addition, by including stands with varying structural characteristics, we assessed whether management-related stand structure differences

modulate gas exchange.

4.1. Seasonal and spatial patterns of gas exchange

Our results showed no effect of stand structure, as reflected by the LAI and basal area of the stands, on needle gas exchange parameters (Tables 2, 3, S2). The fact that gas exchange measurements are typically performed on the upper tree canopy, in combination with the sparse canopy of *P. brutia* and *P. halepensis* that allows the penetration of light deeper in the foliage, could partially explain the lack of any LAI effects of needle gas exchange. This is further supported by the similar A_{max} values between sunlit and shaded needles (Figure S3), which verify an efficient photosynthetic acclimation (Niinemets, 2006; Valladares and Niinemets, 2008) and the absence of any LAI-induced shading effects on A_{max} .

Table 2
Final mixed effect model for Amax.

Predictors	Amax		
	Estimates	CI	p
(Intercept)	4.02	1.03 – 7.02	0.009
VPD mean	-0.95	-1.60 – -0.29	0.005
LSWI	10.88	1.31 – 20.45	0.026
Site [Sani]	9.88	7.25 – 12.50	< 0.001
Site [Xanthi]	8.28	6.11 – 10.44	< 0.001
Season [Spring]	6.46	4.72 – 8.20	< 0.001
Season [Summer]	3.16	0.01 – 6.32	0.049
Season [Autumn]	-1.20	-3.06 – 0.66	0.206
Site [Sani] × Season [Spring]	-0.34	-2.76 – 2.09	0.785
Site [Xanthi] × Season [Spring]	3.67	1.09 – 6.24	0.005
Site [Sani] × Season [Summer]	-2.57	-6.24 – 1.10	0.170
Site [Xanthi] × Season [Summer]	-5.94	-9.80 – -2.08	0.003
Site [Sani] × Season [Autumn]	-1.73	-4.46 – 1.00	0.214
Site [Xanthi] × Season [Autumn]	7.92	5.33 – 10.50	< 0.001
VPD mean × Site [Sani]	-2.64	-4.28 – -1.01	0.002
VPD mean × Site [Xanthi]	0.11	-0.88 – 1.10	0.826
Random Effects			
σ^2	9.03		
τ_{00} Plot	0.79		
ICC	0.08		
N _{plot}	10		
Observations	401		
Marginal R ² / Conditional R ²	0.793 / 0.809		

It can also not be excluded that focusing on dominant trees may have masked potential stand structure-induced competition effects among the pines for soil water. Still, this seems to be less important, given the less pronounced effect of LSWI on photosynthetic capacity and water use efficiency.

While we captured clear seasonal differences in A_{max} , g_s , and iWUE (Fig. 3a, b, c), we acknowledge that performing gas exchange assessments at a higher frequency and longer duration would allow us to more accurately monitor seasonal dynamics. Nevertheless, in both *P. halepensis* in Sani and *P. brutia* in Xanthi, a bimodal photosynthetic activity pattern was evident (Fig. 3a), characterized by a spring peak and a recovery during autumn or winter. This is consistent with previous studies reporting bimodal seasonal dynamics, including *P. halepensis* (Fotelli et al., 2019) and *P. brutia* (Michelozzi et al., 2008), and aligns with broader evidence of bimodal growth patterns under Mediterranean climates (e.g., Tumajer et al., 2022; Valeriano et al., 2023). Bimodal growth, referring to the occurrence of two distinct periods of growth within a year, is an adaptation strategy of woody plants under dry climates. In Mediterranean ecosystems, tree growth activity responds to periods of favorable wet and warm climatic conditions, which may occur not only during spring but also in autumn or winter (Camarero et al., 2010; Campelo et al., 2018; Fotelli et al., 2019, 2020). However, this pattern may vary depending on local microclimate and interannual shifts in precipitation (Pacheco et al., 2016; Tumajer et al., 2021; Valeriano et al., 2023).

In contrast, *P. brutia* in Lesvos showed a more conservative year-round pattern, with generally lower values, compared to the other sites, and a peak in photosynthetic activity only in spring (Fig. 3a). However, a peak of photosynthetic assimilation in *P. brutia* has been reported even in late summer, such as in August (Awada et al., 2003), highlighting the plasticity of the species' photosynthetic responses to local microclimate. In Lesvos, being characterized by the highest VPD among all sites (Fig. 4), the lack of photosynthetic recovery in *P. brutia* after summer could be driven by the combination of persisting high VPD and low LSWI in autumn, which may constrain water transport, stomatal conductance, and photosynthesis (Balducci et al., 2013; Rehschuh et al., 2020).

4.2. Shared isohydric regulation and hydraulic safety

Despite the differences among seasons and sites, both species showed an overall negative response of gas exchange parameters to VPD consistent with isohydric regulation and drought avoidance strategies (Grossiord et al., 2020). Concurrently, iWUE increased with VPD (Fig. 6c), indicating an adaptive trade-off favoring water conservation at the expense of carbon assimilation (Flexas et al., 2013). These coordinated adjustments reflect substantial phenotypic plasticity and the ability of both species to maintain hydraulic safety under increasing evaporative demand (Anderegg et al., 2016; Klein et al., 2011).

This pattern aligns with recent analyses indicating that pines commonly rely on early stomatal closure under drought, reflecting isohydric regulation across broad climatic gradients (Singh et al., 2025). Ecosystem-scale analyses further support this framework, showing that carbon uptake dynamics in drylands are primarily constrained by atmospheric demand while soil moisture plays a secondary role (Jin et al., 2024; Li et al., 2025; Wang et al., 2025). Such a behavior is consistent with the general hydraulic response of pines, where the limited variation in xylem resistance to cavitation leads to a greater emphasis on stomatal regulation as the primary expression for drought response diversity among species (Martínez-Vilalta et al., 2004).

Meta-analyses across tree species indicate that hydraulic safety margins and xylem vulnerability to embolism are main predictors of drought-induced mortality, highlighting that stomatal regulation becomes the primary mechanism mitigating hydraulic failure when hydraulic plasticity is limited (Anderegg et al., 2016; Serrano-León et al., 2025). Furthermore, a recent global meta-analysis demonstrated that plastic adjustments in hydraulic safety traits are generally insufficient to offset increasingly negative leaf water potentials under drought, highlighting the role of stomatal regulation in controlling hydraulic risk (Ramírez-Valiente et al., 2025). In Mediterranean ecosystems, pines tend to adopt drought-avoidance strategies during summer droughts, increasing the risk of carbon limitation under extreme conditions (Aranda et al., 2024).

4.3. Species-specific differences in photosynthetic capacity and hydraulic safety

Nevertheless, under escalating atmospheric drought during the summer, the A_{max} of *P. brutia* was only slightly decreasing in response to the increasing VPD, both in Xanthi and Lesvos (Fig. 5a). At the same period, a notable sharp decline in photosynthetic capacity was observed in *P. halepensis* within a much narrower gradient of VPD. This suggests a lower sensitivity of the photosynthetic performance of *P. brutia* to increasing atmospheric water demand and a more risk-tolerant operating strategy to maintain carbon gain even potentially closer to hydraulic limits.

This is further supported by the lower minimum Ψ_{midday} values we detected in *P. brutia* (on average -3.3 MPa), compared to *P. halepensis* (-2.8 MPa). At this threshold of Ψ_{midday} , stomatal closure occurs in *P. halepensis*, with a hydraulic safety margin of ~ 0.3 MPa between closure and 50 % loss of conductivity (Klein et al., 2011). This is consistent with the steep decline of A_{max} and iWUE of *P. halepensis* as atmospheric and soil drought increased during the summer. Accordingly, *P. halepensis* has been placed toward the stomatal-sensitive end of the isohydric-anisohydric continuum (i.e., more isohydric) (Klein, 2014), compared to *P. brutia*.

Physiological studies on *P. halepensis*, reported early stomatal closure, showing a highly sensitive stomatal control of carbon assimilation under water stress, supporting isohydric regulation (e.g., Melzack et al., 1985; Manzanera et al., 2016), even at juvenile developmental stage (Ghazghazi et al., 2022). Hydraulic trait assessments under a semi-arid environment further indicate that *P. halepensis* maintains a slightly wider hydraulic safety margin than *P. brutia*, suggesting a more conservative hydraulic operation under droughts (Cherif et al., 2019). In

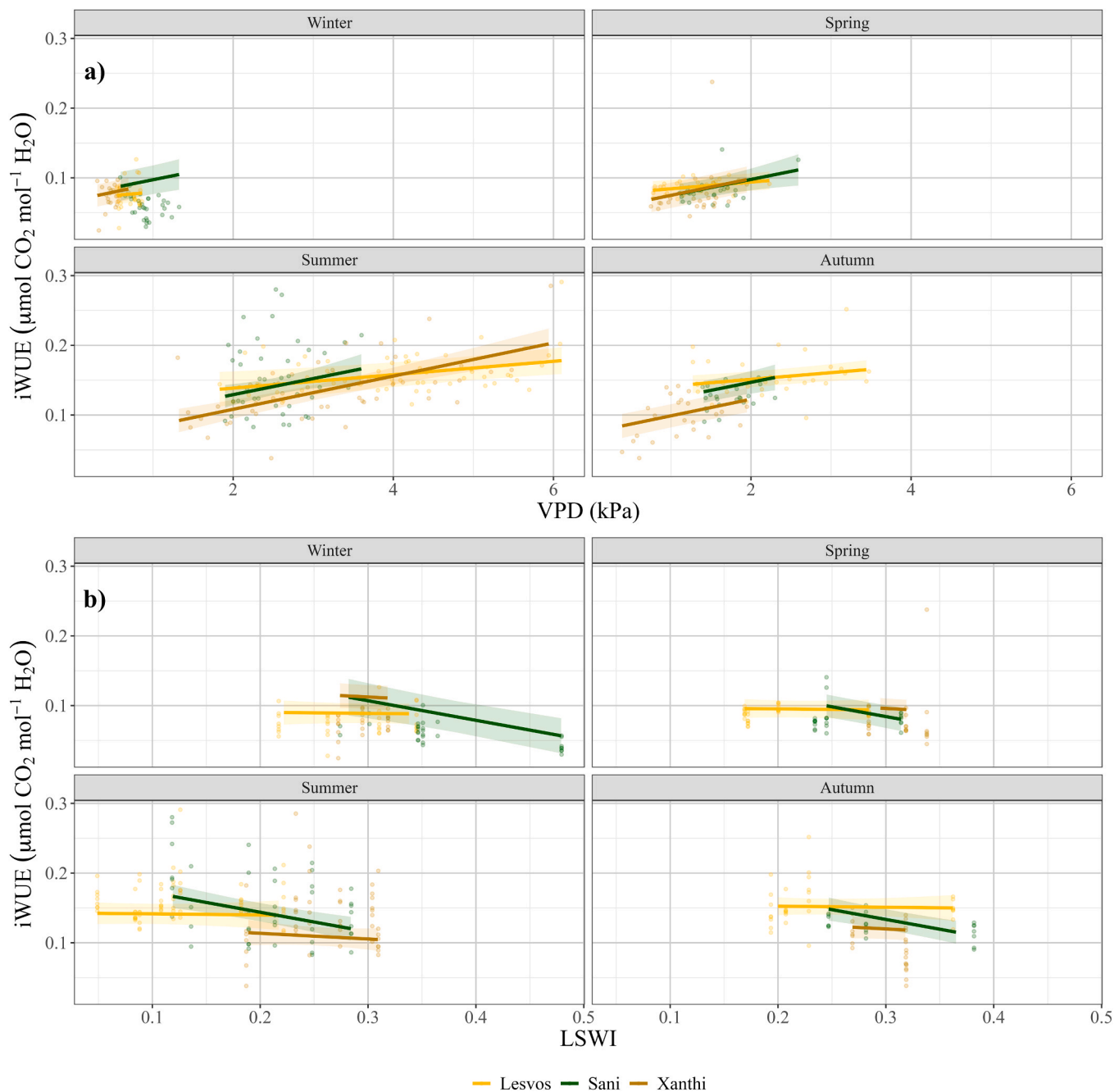


Fig. 6. Relationship between intrinsic Water Use Efficiency (iWUE) and VPD (a) and *Amax* and LSWI (b). Background dots represent the raw data; lines are from the fixed-effect model output and 95 % Confidence Interval ribbons.

accordance with this, post-drought assessments of *P. halepensis* link the hydraulic dysfunction to mortality risk, consistent with its conservative hydraulic operation and sharp summer *Amax* decline (Morcillo et al., 2022).

Although hydraulic safety margins do not directly define isohyricity, those differences provide context supporting our observations of differences in the isohyric response of the two species. Such a conservative water-use strategy by *P. halepensis* vs. *P. brutia*, prioritizing hydraulic safety, may come at the cost of reduced carbon assimilation and growth under prolonged and intense drought (McDowell et al., 2008; Choat et al., 2018).

5. Conclusions

Across a range of climatic and stand structure conditions, *P. halepensis* and *P. brutia* share similar photosynthetic trait responses under dry conditions. Both species are more sensitive to increasing atmospheric drought than to soil and vegetation water limitation and respond by limiting their photosynthetic capacity and increasing their intrinsic water use efficiency. In addition, both species can exhibit a bimodal peak in photosynthetic capacity in spring and after summer drought, when atmospheric demand is not high enough to inhibit the recovery of stomatal conductance. Despite these shared responses, *P. halepensis* shows a stronger sensitivity of photosynthetic capacity to VPD than *P. brutia*, indicating a more isohyric response even at less intense atmospheric drought conditions. In contrast, *P. brutia* maintains

Table 3
Final mixed effect model for iWUE.

Predictors	i WUE		
	Estimates	CI	p
(Intercept)	0.07	0.04 – 0.11	< 0.001
VPD mean	0.01	0.00 – 0.02	0.002
LSWI	-0.02	-0.14 – 0.11	0.806
Site [Sani]	0.07	0.01 – 0.13	0.027
Site [Xanthi]	0.01	-0.05 – 0.08	0.679
Season [Spring]	0.00	-0.01 – 0.02	0.590
Season [Summer]	0.05	0.02 – 0.08	0.005
Season [Autumn]	0.06	0.04 – 0.08	< 0.001
Site [Sani] × Season [Spring]	-0.03	-0.06 – 0.00	0.067
Site [Xanthi] × Season [Spring]	-0.02	-0.05 – 0.00	0.092
Site [Sani] × Season [Summer]	-0.04	-0.09 – 0.01	0.121
Site [Xanthi] × Season [Summer]	-0.06	-0.10 – -0.01	0.009
Site [Sani] × Season [Autumn]	-0.04	-0.06 – -0.01	0.017
Site [Xanthi] × Season [Autumn]	-0.05	-0.08 – -0.03	< 0.001
VPD mean × Site [Sani]	0.01	-0.00 – 0.03	0.136
VPD mean × Site [Xanthi]	0.01	0.00 – 0.02	0.003
LSWI × Site [Sani]	-0.27	-0.44 – -0.09	0.003
LSWI × Site [Xanthi]	-0.07	-0.29 – 0.16	0.559
Random Effects			
σ^2	0.00		
τ_{00} Plot	0.00		
ICC	0.04		
N _{Plot}	10		
Observations	397		
Marginal R ² / Conditional R ²	0.652 / 0.666		

its photosynthetic capacity under elevated VPD, suggesting greater tolerance to atmospheric drought, which is in line with recent findings indicating that *P. brutia* outperforms *P. halepensis* in terms of survival and growth under the same drought conditions (Veuillen et al., 2023). Our results highlight the capacity of both Mediterranean pines for physiological adjustments to withstand drought conditions but also identify differences in the isohydric range of the two species. These insights contribute to our better understanding of how these two species balance carbon gain and water use under increasing droughts that are critical for predicting forest functioning and informing management decisions in the eastern Mediterranean region under intensifying drought.

CRedit authorship contribution statement

Rossella Guerrieri: Writing – review & editing. **Mariangela N. Fotelli:** Writing – review & editing, Supervision, Methodology, Conceptualization. **Christodoulos Sazeides:** Writing – review & editing, Methodology, Data curation. **Nikos Markos:** Writing – review & editing, Methodology, Formal analysis, Data curation. **Alexandros Gouvas:** Methodology, Data curation. **Evdoxia Bintsi-Frantzi:** Writing – review & editing, Methodology, Data curation. **Efstathia D. Mantzari:** Writing – review & editing, Methodology, Data curation. **Georgios Xanthopoulos:** Writing – review & editing, Methodology, Data curation. **Panayiotis G. Dimitrakopoulos:** Writing – review & editing, Supervision, Methodology, Conceptualization. **Nikolaos M. Fyllas:** Writing – review & editing, Supervision, Methodology, Conceptualization. **Gavriil Spyroglou:** Writing – review & editing, Supervision, Methodology. **Kalliopi Radoglou:** Writing – review & editing, Supervision, Methodology, Conceptualization. **Natasa Kiorapostolou:** Writing – original draft, Methodology, Formal analysis, Data curation. **Nikoleta Eleftheriadou:** Writing – original draft, Methodology, Data curation.

Funding

This work is part of the “PineOptim” project, which is implemented in the framework of H.F.R.I. call “Basic Research Financing (Horizontal support of all Sciences)” under the National Recovery and Resilience

Plan “Greece 2.0” funded by the European Union – NextGenerationEU (H.F.R.I. Project Number: 016258).

Declaration of Competing Interest

The authors declare the following financial interests/personal relationships which may be considered as potential competing interests: Natasa Kiorapostolou, Nikoleta Eleftheriadou, Christodoulos Sazeides, Nikos Markos, Alexandros Gouvas, Evdoxia Bintsi-Frantzi, Efstathia D. Mantzari, Georgios Xanthopoulos, Panayiotis G. Dimitrakopoulos, Gavriil Spyroglou, Kalliopi Radoglou, Mariangela N. Fotelli reports financial support was provided by Hellenic Foundation for Research and Innovation. If there are other authors, they declare that they have no known competing financial interests or personal relationships that could have appeared to influence the work reported in this paper.

Appendix A. Supporting information

Supplementary data associated with this article can be found in the online version at doi:10.1016/j.foreco.2026.123614.

Data availability

Data will be made available on request.

References

- Alsanousi, A.A., Abdul-Hamid, H., Mohamed, J., Masoud, M., 2025. *Pinus halepensis* Mill. in the Mediterranean region: a review of ecological significance, growth patterns, and soil interactions. *iForest* 18, 30.
- Anderegg, W.R., Klein, T., Bartlett, M., Sack, L., Pellegrini, A.F., Choat, B., Jansen, S., 2016. Meta-analysis reveals that hydraulic traits explain cross-species patterns of drought-induced tree mortality across the globe. *Proc. Natl. Acad. Sci.* 113, 5024–5029.
- Aranda, I., Martín-Benito, D., Sánchez-Gómez, D., de Simón, B.F., Gea-Izquierdo, G., 2024. Different drought-tolerance strategies of tree species to cope with increased water stress under climate change in a mixed forest. *Physiol. Plant* 176, e14562.
- Awada, T., Radoglou, K., Fotelli, M.N., Constantinidou, H.I., 2003. Ecophysiology of seedlings of three Mediterranean pine species in contrasting light regimes. *Tree Physiol.* 23, 33–41.
- Balducci, L., Deslauriers, A., Giovannelli, A., Rossi, S., Rathgeber, C.B., 2013. Effects of temperature and water deficit on cambial activity and woody ring features in *Picea mariana* saplings. *Tree Physiol.* 33, 1006–1017.
- Bates, D., Mächler, M., Bolker, B., Walker, S., 2015. Fitting linear mixed-effects models using lme4. *J. Stat. Softw.* 67, 1–48.
- Birami, B., Gattmann, M., Heyer, A.G., Grote, R., Arnecht, A., Ruehr, N.K., 2018. Heat waves alter carbon allocation and increase mortality of Aleppo pine under dry conditions. *Front. For. Glob. Change* 1, 8.
- Camarero, J.J., Olano, J.M., Perras, A., 2010. Plastic bimodal xylogenesis in conifers from continental Mediterranean climates. *N. Phytol.* 185, 471–480.
- Campelo, F., Gutiérrez, E., Ribas, M., Sanchez-Salguero, R., Nabais, C., Camarero, J.J., 2018. The facultative bimodal growth pattern in *Quercus ilex* – a simple model to predict sub-seasonal and inter-annual growth. *Dendrochronologia* 49, 77–88.
- Chambel, M.R., Climent, J., Pichot, C., Ducci, F., 2013. Mediterranean pines (*Pinus halepensis* Mill. and *Pinus brutia* Ten.). In: Pâques, L.E. (Ed.), *Forest tree breeding in Europe: current state-of-the-art and perspectives*. Springer, Cham, pp. 229–265.
- Cherif, S., Ezzine, O., Khouja, M.L., Nasr, Z., 2019. Hydraulic traits performances of three pine species in Tunisia. *J. Agric. Sci.* 11, 1–20.
- Choat, B., Brodribb, T.J., Brodersen, C.R., Duursma, R.A., López, R., Medlyn, B.E., 2018. Triggers of tree mortality under drought. *Nature* 558, 531–539.
- Christopoulou, A., Sazeides, C.I., Fyllas, N.M., 2022. Size-mediated effects of climate on tree growth and mortality in Mediterranean *Brutia* pine forests. *Sci. Total Environ.* 812, 151463.
- Eleftheriadou, N., Mantzari, E.D., Kiorapostolou, N., Sazeides, C.I., Xanthopoulos, G., Markos, N., et al., 2026. An integrated monitoring protocol to study the effects of management on the C sequestration potential of Mediterranean pine ecosystems. *Methods Protoc.* 9, 18.
- Farquhar, G.D., Sharkey, T.D., 1982. Stomatal conductance and photosynthesis. *Annu. Rev. Plant Physiol.* 33, 317–345.
- Flexas, J., Niinemets, Ü., Gallé, A., Barbour, M.M., Centritto, M., Diaz-Espejo, A., Douthe, C., Galmés, J., Ribas-Carbo, M., Rodriguez, P.L., Rosselló, F., Soolanayakanahally, R., Tomas, M., Wright, I.J., Farquhar, G.D., Medrano, H., 2013. Diffusional conductances to CO₂ as a target for increasing photosynthesis and photosynthetic water-use efficiency. *Photosynth. Res.* 117, 45–59.
- Fotelli, M.N., Korakaki, E., Paparrizos, S.A., Radoglou, K., Awada, T., Matarakis, A., 2019. Environmental controls on the seasonal variation in gas exchange and water balance in a near-coastal Mediterranean *Pinus halepensis* forest. *Forests* 10, 313.

- Fotelli, M.N., Lyrou, F.G., Avtzis, D.N., Maurer, D., Rennenberg, H., Spyroglou, G., Polle, A., Radoglou, K., 2020. Effective defense of Aleppo pine against the giant scale *Marchalina hellenica* through ecophysiological and metabolic changes. *Front. Plant Sci.* 11, 581693. <https://doi.org/10.3389/fpls.2020.581693>.
- Fyllas, N.M., Christopoulou, A., Galanidis, A., Michelaki, C., Dimitrakopoulos, P.G., Fule, P.Z., et al., 2017. Tree growth–climate relationships in a forest–plot network on Mediterranean mountains. *Sci. Total Environ.* 598, 393–403. <https://doi.org/10.1016/j.scitotenv.2017.04.145>.
- Fyllas, N.M., Michelaki, C., Galanidis, A., Evangelou, E., Zaragoza-Castells, J., Dimitrakopoulos, P.G., et al., 2020. Functional trait variation among and within species and plant functional types in mountainous Mediterranean forests. *Front. Plant Sci.* 11, 212. <https://doi.org/10.3389/fpls.2020.00212>.
- Ghazghazi, H., Riahi, L., Yangui, I., Messaoud, C., Rzigui, T., Nasr, Z., 2022. Effect of drought stress on physio-biochemical traits and secondary metabolites production in the woody species *Pinus halepensis* Mill. at a juvenile development stage. *J. Sustain. For.* 41, 878–894.
- Grossiord, C., Buckley, T.N., Cernusak, L.A., Novick, K.A., Poulter, B., Siegwolf, R.T., Sperry, J.S., McDowell, N.G., 2020. Plant responses to rising vapor pressure deficit. *N. Phytol.* 226, 1550–1566.
- Houminer, N., Riov, J., Moshellon, M., Osem, Y., David-Schwartz, R., 2022. Comparison of morphological and physiological traits between *Pinus brutia*, *Pinus halepensis*, and their vigorous F1 hybrids. *Forests* 13, 1747.
- IPCC, 2023. In: Lee, H., Romero, J. (Eds.), Summary for Policymakers. In: *Climate Change 2023: Synthesis Report. Contribution of Working Groups I, II and III to the Sixth Assessment Report of the Intergovernmental Panel on Climate Change*. IPCC, Geneva, Switzerland, pp. 1–34. <https://doi.org/10.59327/IPCC/AR6-9789291691647.001> (Core Writing Team).
- Jin, C., Zha, T., Bourque, C.P., Jia, X., Tian, Y., Liu, P., Li, X., Xu, M., Guo, Z., Hu, Z., 2024. Ecosystem-scale carbon dynamics in desert shrublands: unraveling the complex interplay among leaf functional and physiological traits and environment. *Agric. For. Meteorol.* 355, 110133.
- Kiorapostolou, N., Galiano-Pérez, L., Von Arx, G., Gessler, A., Petit, G., 2018. Structural and anatomical responses of *Pinus sylvestris* and *Tilia platyphyllos* seedlings exposed to water shortage. *Trees* 32, 1211–1218.
- Klein, T., 2014. The variability of stomatal sensitivity to leaf water potential across tree species indicates a continuum between isohydric and anisohydric behaviours. *Func. Ecol.* 28, 1313–1320.
- Klein, T., Cohen, S., Yakir, D., 2011. Hydraulic adjustments underlying drought resistance of *Pinus halepensis*. *Tree Physiol.* 31, 637–648.
- Kuznetsova, A., Brockhoff, P.B., Christensen, R.H.B., 2017. lmerTest package: tests in linear mixed effects models. *J. Stat. Softw.* 82, 1–26.
- Lawson, T., Blatt, M.R., 2014. Stomatal size, speed, and responsiveness impact on photosynthesis and water use efficiency. *Plant Physiol.* 164, 1556–1570.
- Lazoglou, G., Papadopoulos-Zachos, A., Georgiades, P., Zittis, G., Velikou, K., Manios, E. M., Anagnostopoulou, C., 2024. Identification of climate change hotspots in the Mediterranean. *Sci. Rep.* 14, 29817.
- Li, C., Zhang, D., Zhang, S., Wen, Y., Wang, W., Chen, Y., Peng, J., 2025. Atmospheric vapor pressure deficit outweighs soil moisture deficit in controlling global ecosystem water use efficiency. *J. Geophys. Res. Biogeosci.* 130.
- Manzanera, J.A., Gómez-Garay, A., Pintos, B., Rodríguez-Rastrero, M., Moreda, E., Zazo, J., Martínez-Falero, E., García-Abril, A., 2016. Sap flow, leaf-level gas exchange and spectral responses to drought in *Pinus sylvestris*, *Pinus pinea* and *Pinus halepensis*. *iForest* 10, 204.
- Markos, N., Kyparissis, A., 2011. Ecophysiological modelling of leaf level photosynthetic performance for three Mediterranean species with different growth forms. *Funct. Plant Biol.* 38, 314–326.
- Markos, N., Preisler, Y., Radoglou, K., Rotenberg, E., Yakir, D., 2024. Physiological and phenological adjustments in water and carbon fluxes of Aleppo pine forests under contrasting climates in the Eastern Mediterranean. *Tree Physiol.* 44, tpad125.
- Martínez-Vilalta, J., García-Fórner, N., 2017. Water potential regulation, stomatal behaviour and hydraulic transport under drought: deconstructing the iso/anisohydric concept. *Plant Cell Environ.* 40, 962–976.
- Martínez-Vilalta, J., Poyatos, R., Aguadé, D., Retana, J., Mencuccini, M., 2014. A new look at water transport regulation in plants. *N. Phytol.* 204, 105–115.
- Martínez-Vilalta, J., Sala, A., Pinol, J., 2004. The hydraulic architecture of Pinaceae – a review. *Plant Ecol.* 171, 3–13.
- McDowell, N., Pockman, W.T., Allen, C.D., Breshears, D.D., Cobb, N., Kolb, T., Palut, J., Sperry, J., West, A., Williams, D.G., Yezzer, E.A., 2008. Mechanisms of plant survival and mortality during drought. *N. Phytol.* 178, 719–739.
- Melzack, R.N., Bravdo, B., Riov, J., 1985. The effect of water stress on photosynthesis and related parameters in *Pinus halepensis*. *Physiol. Plant* 64, 295–300.
- Michelozzi, M., Tognetti, R., Maggino, F., Radicati, M., 2008. Seasonal variations in monoterpene profiles and ecophysiological traits in Mediterranean pine species of group “*halepensis*”. *iForest* 1, 65.
- Miner, G.L., Bauerle, W.L., Baldocchi, D.D., 2017. Estimating the sensitivity of stomatal conductance to photosynthesis: a review. *Plant Cell Environ.* 40, 1214–1238.
- Morcillo, L., Muñoz-Rengifo, J.C., Torres-Ruiz, J.M., Delzon, S., Moutahir, H., Vilagrosa, A., 2022. Post-drought conditions and hydraulic dysfunction determine tree resilience and mortality across Mediterranean Aleppo pine (*Pinus halepensis*) populations after an extreme drought event. *Tree Physiol.* 42, 1364–1376.
- Moreno-Fernandez, D., Díaz-Pinés, E., Barbeito, I., Sanchez-Gonzalez, M., Montes, F., Rubio, A., Cañellas, I., 2015. Temporal carbon dynamics over the rotation period of two alternative management systems in Mediterranean mountain Scots pine forests. *For. Ecol. Manag.* 348, 186–195.
- Navarro-Cerrillo, R.M., Ruiz-Gómez, F.J., Camarero, J.J., Castillo, V., Barberá, G.G., Palacios-Rodríguez, G., Navarro, F.B., Blanco, J.A., Imbert, J.B., Cachinero-Vivar, A. M., Molina, A.M., del Campo, A.D., 2022. Long-term carbon sequestration in pine forests under different silvicultural and climatic regimes in Spain. *Forests* 13, 450.
- Niinemets, Ü., 2006. The controversy over traits conferring shade-tolerance in trees: ontogenetic changes revisited. *J. Ecol.* 94, 464–470.
- Niinemets, Ü., 2010. Responses of forest trees to single and multiple environmental stresses from seedlings to mature plants. *For. Ecol. Manag.* 260, 1623–1639.
- Pacheco, A., Camarero, J.J., Carrer, M., 2016. Linking wood anatomy and xylogenesis allows pinpointing of climate and drought influences on growth of coexisting conifers. *Tree Physiol.* 36, 502–512.
- Penuelas, J., Sardans, J., Filella, I., Estiarte, M., Llusià, J., Ogaya, R., Carnicer, J., Bartrons, M., Rivas-Ubach, A., Grau, O., Peguero, G., Margalef, O., Pla-Rabes, S., Stefanescu, C., Asensio, D., Preece, C., Liu, L., Verger, A., Barbata, A., Achotegui-Castells, A., Terradas, J., 2017. Impacts of global change on Mediterranean forests and their services. *Forests* 8, 463.
- R Core Team, 2024. *R: A language and environment for statistical computing*. R Foundation for Statistical Computing, Vienna, Austria. (<https://www.R-project.org/>).
- Ramírez-Valiente, J.A., Poyatos, R., Blackman, C.J., Cabon, A., Castells, E., Cochard, H., Creek, D., Delzon, S., García-Valdés, R., Limousin, J.-M., López, R., Martin-StPaul, N., Mencuccini, M., 2025. Limited plastic responses in safety traits support greater hydraulic risk under drier conditions. *Nat. Ecol. Evol.* 9, 1825–1836.
- Rehseh, R., Cecilia, A., Zuber, M., Faragó, T., Baumbach, T., Hartmann, H., Jansen, S., Mayr, S., Ruehr, N., 2020. Drought-induced xylem embolism limits the recovery of leaf gas exchange in Scots pine. *Plant Physiol.* 184, 852–864.
- del Río, M., et al., 2017. Mediterranean pine forests: management effects on carbon stocks. In: Bravo, F., LeMay, V., Jandl, R. (Eds.), *Managing Forest Ecosystems: The Challenge of Climate Change*. Manag. For. Ecosyst., vol. 34. Springer, Cham. https://doi.org/10.1007/978-3-319-28250-3_15.
- Sarris, D., Christodoulakis, D., Körner, C., 2007. Recent decline in precipitation and tree growth in the eastern Mediterranean. *Glob. Change Biol.* 13, 1187–1200.
- Sazeides, C.I., Christopoulou, A., Fyllas, N.M., 2021. Coupling photosynthetic measurements with biometric data to estimate gross primary productivity (GPP) in Mediterranean pine forests of different post-fire age. *Forests* 12, 1256.
- Sazeides, C.I., Fyllas, N.M., 2025. Simulating Net Ecosystem Productivity (NEP) in Mediterranean Pine Forests (*Pinus brutia*) During the 21st Century: The Effect of Leaf Area Index and Elevation. *Plants* 14 (7), 1090.
- Schneider, C.A., Rasband, W.S., Eliceiri, K.W., 2012. NIH Image to ImageJ: 25 years of image analysis. *Nat. Methods* 9, 671–675.
- Serrano-León, H., Blondeel, H., Glenz, P., Steurer, J., Schnabel, F., Baeten, L., Guillemot, J., Martin-StPaul, N., Skiadaresis, G., Scherer-Lorenzen, M., Bonal, D., 2025. Multiyear drought strengthens positive and negative functional diversity effects on tree growth response. *Glob. Change Biol.* 31, e70394.
- Singh, S.P., Gumber, S., Singh, R.D., Li, T., Pandey, R., 2025. A global comparative analysis of drought responses of pines and oaks. *Forests* 16, 1660.
- Tatarinov, F., Rotenberg, E., Maseyk, K., Ogée, J., Klein, T., Yakir, D., 2016. Resilience to seasonal heat wave episodes in a Mediterranean pine forest. *N. Phytol.* 210, 485–496.
- Tumajer, J., Serra-Malquer, X., Gazol, A., de Andrés, E.G., Colangelo, M., Sangüesa-Barreda, G., Olano, J.M., Rozas, V., García-Plazaola, J.I., Fernández-Marín, B., Imbert, B., Coll, L., Ameztegui, A., Espelta, J.M., Alla, A.Q., Campelo, F., Camarero, J.J., 2022. Bimodal and unimodal radial growth of Mediterranean oaks along a coast-inland gradient. *Agric. For. Meteorol.* 327, 109234.
- Tumajer, J., Shishov, V.V., Ilyin, V.A., Camarero, J.J., 2021. Intra-annual growth dynamics of Mediterranean pines and junipers determines their climatic adaptability. *Agric. For. Meteorol.* 311, 108685.
- Valeriano, C., Gutiérrez, E., Colangelo, M., Gazol, A., Sánchez-Salguero, R., Tumajer, J., Shishov, V., Bonet, J.A., Martínez de Aragón, J., Ibáñez, R., Valerio, M., Camarero, J. J., 2023. Seasonal precipitation and continentality drive bimodal growth in Mediterranean forests. *Dendrochronologia* 78, 126057.
- Valladares, F., Niinemets, Ü., 2008. Shade tolerance, a key plant feature of complex nature and consequences. *Annu. Rev. Ecol. Syst.* 39, 237–257.
- Veuillen, L., Prévosto, B., Zeoli, L., Pichot, C., Cailleret, M., 2023. *Pinus halepensis* and *P. brutia* provenances present similar resilience to drought despite contrasting survival, growth, cold tolerance and stem quality. *For. Ecol. Manag.* 544, 121146.
- Wang, M., Wang, Y., Liu, X., Hou, W., Wang, J., Li, S., Zhao, L., Hu, Z., 2025. Vapor pressure deficit dominates vegetation productivity during compound drought and heatwave events in China’s arid and semi-arid regions: evidence from multiple vegetation parameters. *Ecol. Inf.* 88, 103144.
- Warren, C.R., 2008. Soil water deficits decrease the internal conductance to CO₂ transfer but atmospheric water deficits do not. *J. Exp. Bot.* 59, 327–334.
- Warren, C.R., Livingston, N.J., Turpin, D.H., 2004. Water stress decreases the transfer conductance of Douglas-fir (*Pseudotsuga menziesii*) seedlings. *Tree Physiol.* 24, 971–979.
- Zhou, S., Duursma, R.A., Medlyn, B.E., Kelly, J.W., Prentice, I.C., 2013. How should we model plant responses to drought? An analysis of stomatal and non-stomatal responses to water stress. *Agric. For. Meteorol.* 182, 204–214.